ACS Combinatorial Science

Article

Intramolecular Electrophilic Cyclization Approach to 6-Substituted Naphtho[2,1-b]benzofurans: Novel Dual-State Emissive Fluorophores with Blue Emission

Dileep Kumar Singh, Kyungkuk Jang, Jinhwang Kim, Jeeyeon Lee, and Ikyon Kim

ACS Comb. Sci., **Just Accepted Manuscript** • DOI: 10.1021/acscombsci.9b00006 • Publication Date (Web): 29 Mar 2019

Just Accepted

ACS Publications

is published by the American Chemical Society. 1155 Sixteenth Street N.W., Washington, DC 20036

Intramolecular Electrophilic Cyclization Approach to 6-Substituted Naphtho[2,1-*b*]benzofurans: Novel Dual-State Emissive Fluorophores with Blue Emission

Dileep Kumar Singh,[a,‡] Kyungkuk Jang,[b‡] Jinhwang Kim,[a] Jeeyeon Lee,*[,b] and Ikyon Kim *[,a]

[a] College of Pharmacy and Yonsei Institute of Pharmaceutical Sciences, Yonsei University 85 Songdogwahak-ro, Yeonsu-gu, Incheon, 21983, Republic of Korea

[b] College of Pharmacy, Research Institute of Pharmaceutical Sciences, Seoul National University, 1 Gwanak-ro, Gwanak-gu, Seoul, 08826, Republic of Korea

‡ These authors contributed equally.

* Corresponding authors.

Tel.: +82 32 749 4515; fax: +82 32 749 4105; e-mail: ikyonkim@yonsei.ac.kr

Tel.: +82 2 880 2471; fax: +82 2 884 8334; e-mail: jyleeut@snu.ac.kr

Table of Contents

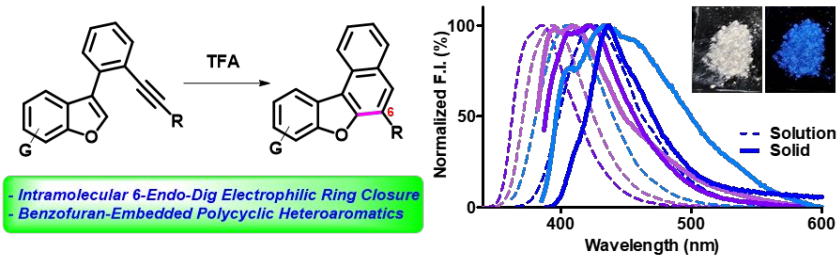

Abstract:

A regiospecific synthesis of naphtho[2,1-*b*]benzofurans with a substituent at the C6 position has been achieved via intramolecular 6-endo-dig electrophilic cyclization under acidic conditions to construct the central aromatic C ring. Screening of the synthesized compounds using a high-content imaging system enabled us to discover novel dual state emissive compounds **2**{*1,6*}, **2**{*1,8*}, and **2**{*4,3*}, which are highly emissive with blue emission in their solid states as well as in solution states in most solvents. In addition, the compounds **2**{*4,3*}, **2**{*4,12*}, and **2**{*5,13*} were found to be the most cell permeable in HeLa cells for live cell imaging with negligible phototoxicity.

Keywords: Naphtho[2,1-*b*]benzofuran; Sonogashira coupling; Intramolecular reaction; Electrophilic reaction; Polycycles; Heteroaromatics; Fluorescence.

Introduction

Polycyclic heteroaromatic compounds represent an important class of organic functional materials with aromaticity exhibiting various biological, electrochemical, and photochemical properties.[1-7] Among the various applications of heteroaromatic scaffolds, the development of novel fluorescent probes is immensely powerful in biomedical research, particularly for bioimaging applications.[8-10] Desirable features of fluorescent probes for bioimaging are better photostability and higher contrast of fluorescence. Aggregation-caused quenching (ACQ) effects of conventional fluorophores, such as pyrene, perylene, and naphthalene diimide (NDI), are detrimental to practical applications in bioimaging, optoelectronic materials, and sensors.[11-13] Aggregation-induced emission (AIE) or Aggregation-induced emission enhancement (AIEE) molecules have shown great potential as a new modality because they are not quenched at high concentrations.[14-18] Nonradiative deactivation pathways observed in solutions can be suppressed by restricted intramolecular rotation (RIR) in highly concentrated solutions or in solid states, leading to a better contrast in fluorescence imaging. To date, a variety of AIE luminogens with their quantum yields (QY) close to unity have been developed, but there still remains a solubility issue in most systems for bioimaging applications, thus requiring nanoparticle fabrication processes for enhanced cellular uptake.[19]

Novel fluorophores with high fluorescence in solution as well as in solid states are highly demanded for bioimaging and biosensors, but such probes are still limited.[20-25] In particular, blue fluorescent materials functioning in solution and solid states are still rare and in high demand for high performance blue OLEDs.[26-28] In addition, dual state emission (DSE) molecules that are emissive in all types of solvents are rarely encountered.[29-31] To overcome the practical limits of conventional fluorophores, extensive synthetic efforts have been

dedicated to identify new polycyclic heteroaromatic scaffolds. The development of novel emissive scaffolds can be more efficiently implemented in combinatorial approaches along with a high content imaging system, since cell permeability, photostability, and cytotoxicity are not predictable from the rational design of biosensors in the context of the cellular system.[4, 32] As part of our continued efforts toward benzofurans,[33-39] we recently became interested in regiospecific construction of benzofuran-containing polycyclic structures.[40-41]

Scheme 1. Synthetic plans

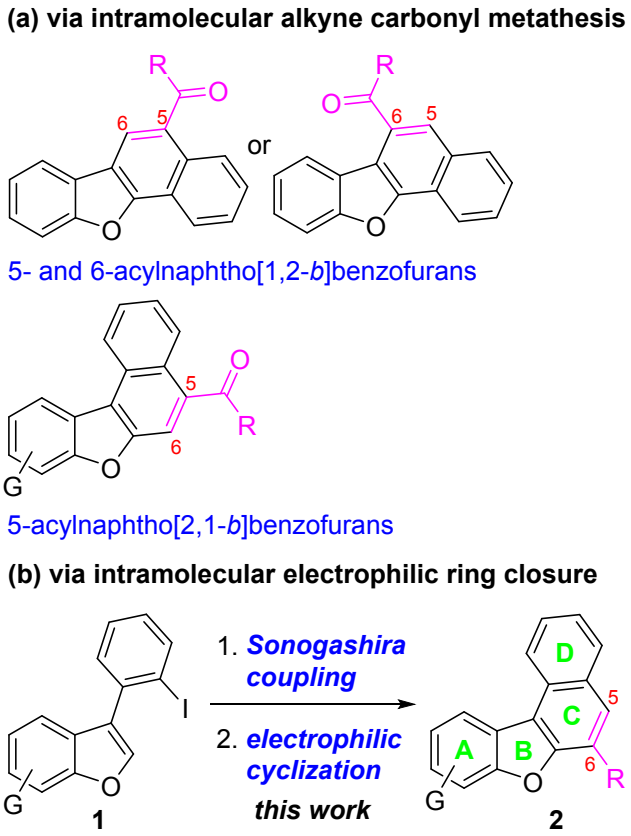

In particular, employing intramolecular alkyne carbonyl metathesis enabled us to install an acyl moiety to naphtho[1,2-*b*]benzofurans or naphtho[2,1-*b*]benzofurans in a regiospecific manner in the course of the central aromatic ring formation (Scheme 1(a)). During this study, we expected that sequential Sonogashira coupling[42-45] and 6-endo-dig electrophilic cyclization[46-

[49] of 3-(2-iodophenyl)benzofurans **(1)** would lead to naphtho[2,1-*b*]benzofurans with a substituent at the C6 position (Scheme 1(b)).[50] Despite the importance of this core skeleton in the area of organic electronic devices,[51-54] only a limited number of synthetic approaches in which expensive metal catalysts and/or harsh reaction conditions were used have appeared in the literature.[55-60] These shortcomings as well as a great interest in furan-fused polycyclic systems for optoelectronic applications[61] encouraged us to evaluate our route to this polycyclic heteroaromatic scaffold, which is the focus of this study.

Results and discussion

For reaction optimization, we used 3-arylbenzofuran **1**{*1*} which was prepared by following the previous procedure.[40, 62] Sonogashira coupling of **1**{*1*} with phenylacetylene **3**{*1*} in the presence of $(Ph_3P)_2PdCl_2$ (0.1 equiv) and CuI (0.1 equiv) in Et_3N at 80 °C afforded **4**{*1,1*}.

Scheme 2. Synthesis of 2{*1*}

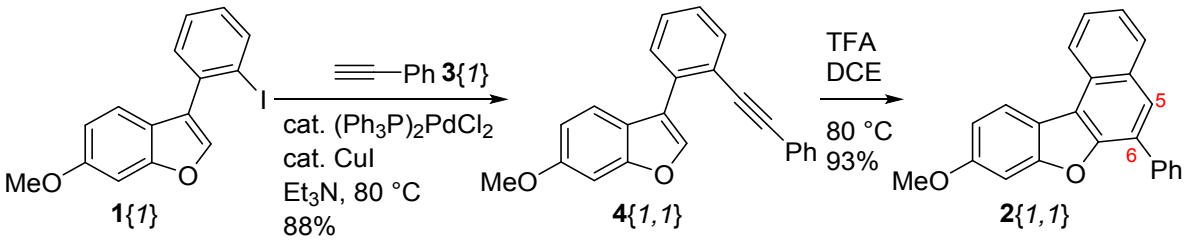

After screening of the several reaction conditions, we found that exposure of **4**{*1,1*} to catalytic amount of $InCl_3$ (0.05 equiv) at 80 °C for 12 h gave the tetracyclic product **2**{*1,1*} in 85% yield. However, full conversion was not observed in some substrates where other alkynes were attached although the reason is not clear. It turned out that $PtCl_2$, $Bi(OTf)_3$, or AgOTf was ineffective in this transformation. Finally, it was discovered that heating of **4**{*1,1*} in TFA/1,2-

dichloroethane (DCE) (=1/2) at 80 °C for 0.5 h cleanly provided the desired **2**{*1,1*} in excellent yield.

Having established the optimal conditions, reaction scope was first examined with substrates **4**{*1,2-9*} with different R groups (Table 1). Benzofurans **1**{*1-6*} and terminal alkynes **3**{*1-13*} for Sonogashira coupling are listed in Figures 1 and 2. Not only electron-rich aryl groups but also electron-poor aryl moiety were well tolerated under these conditions to afford the corresponding 6-arylnaphtho[2,1-*b*]benzofurans in good to excellent yields (entries 1-6). A naphtho[2,1-*b*]benzofuran-bearing heterocycle such as thiophene was also produced in 63% yield (entry 7). However, only a trace amount of the product was obtained with alkyl-substituted benzofuran **4**{*1,9*} (entry 8). Next, this sequence was applied to the other benzofurans **1**{*2-6*}[63] with different alkynes to further demonstrate a wide substrate scope (entries 9-19). Overall, the desired tetracyclic skeletons were established in good overall yields without side products.

Figure 1. Benzofurans 1{*1-6*}

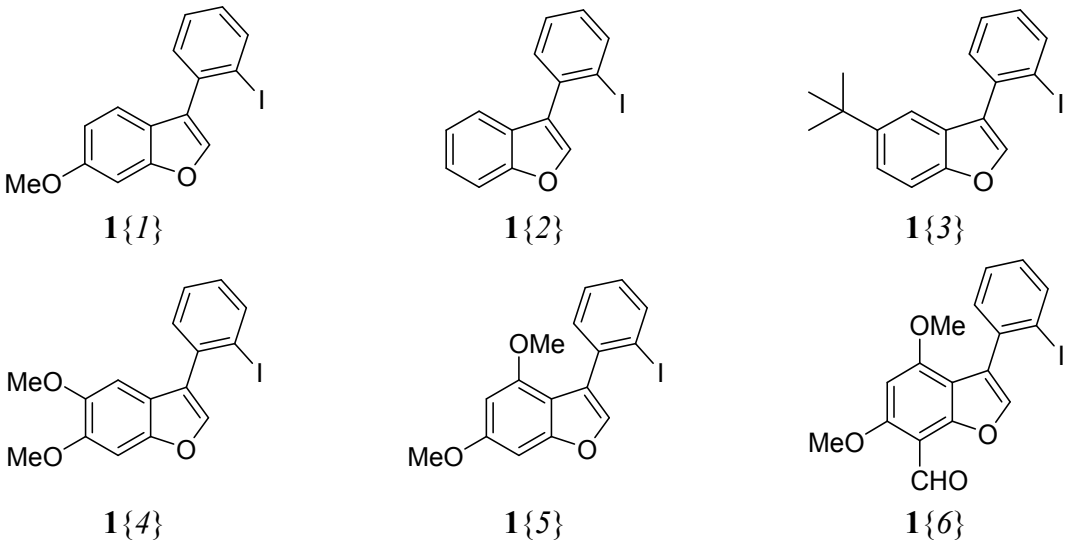

1{*1*} **1**{*2*} **1**{*3*}

1{*4*} **1**{*5*} **1**{*6*}

Figure 2. Terminal Alkynes 3{*1-13*}

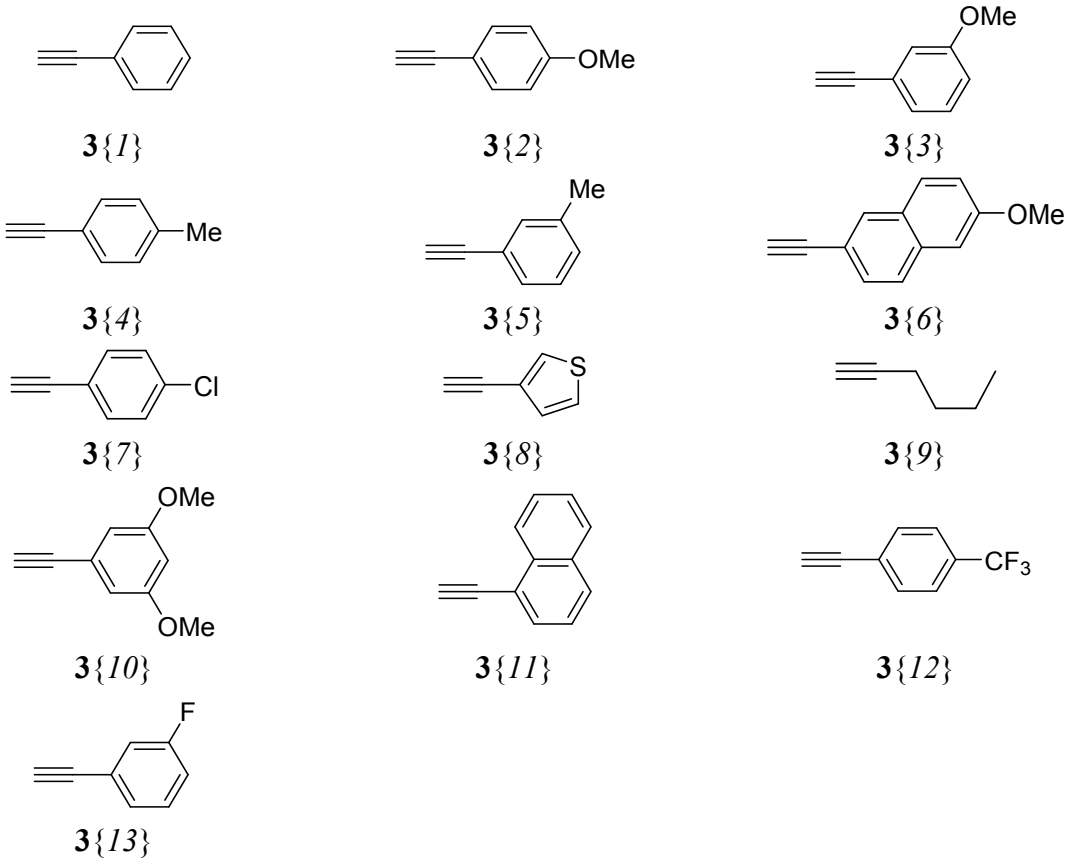

3{*1*} **3**{*2*} **3**{*3*}

3{*4*} **3**{*5*} **3**{*6*}

3{*7*} **3**{*8*} **3**{*9*}

3{*10*} **3**{*11*} **3**{*12*}

3{*13*}

Table 1. Synthesis of Diverse 6-Substituted Naphtho[2,1-*b*]benzofurans[a]

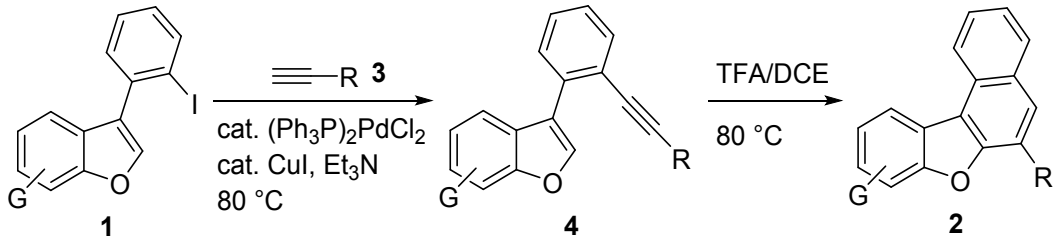

1 **4** **2**

entry	**1**	alkyne	**4**[b]	**2**[b]
1	**1**{*1*}	**3**{*2*}	**4**{*1,2*} (85)	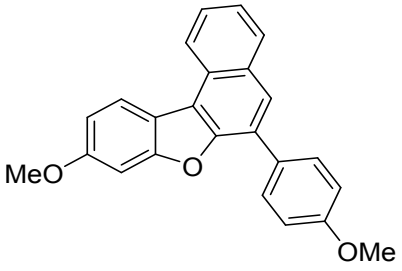 **2**{*1,2*} (88)

2	**1**{*1*}	**3**{*3*}	**4**{*1,3*} (83)	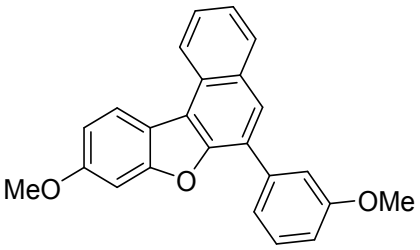	**2**{*1,3*} (90)
3	**1**{*1*}	**3**{*4*}	**4**{*1,4*} (90)	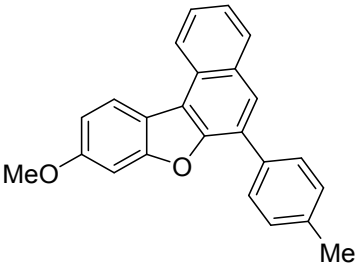	**2**{*1,4*} (78)
4	**1**{*1*}	**3**{*5*}	**4**{*1,5*} (91)	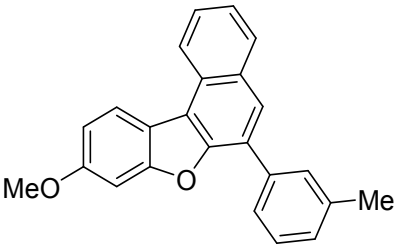	**2**{*1,5*} (86)
5	**1**{*1*}	**3**{*6*}	**4**{*1,6*} (78)	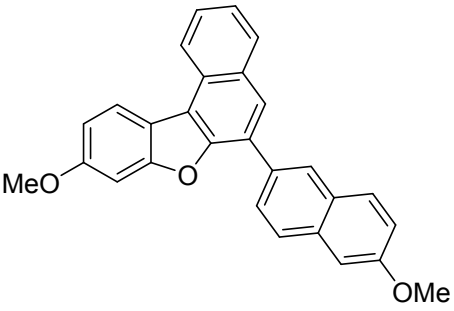	**2**{*1,6*} (76)
6	**1**{*1*}	**3**{*7*}	**4**{*1,7*} (80)	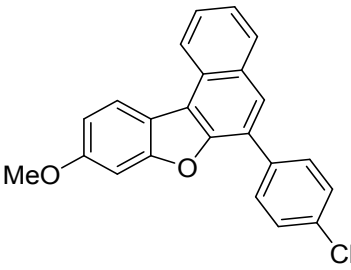	**2**{*1,7*} (74)
7	**1**{*1*}	**3**{*8*}	**4**{*1,8*} (83)	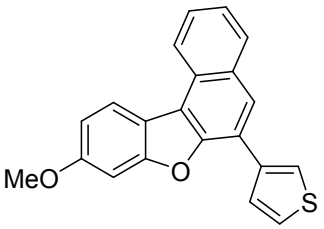	**2**{*1,8*} (63)
8	**1**{*1*}	**3**{*9*}	**4**{*1,9*} (98)	trace	**2**{*1,9*}

9	**1**{*2*}	**3**{*1*}	**4**{*2,1*} (92)	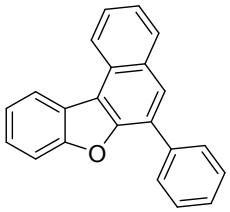	**2**{*2,1*} (77)
10	**1**{*2*}	**3**{*7*}	**4**{*2,7*} (66)	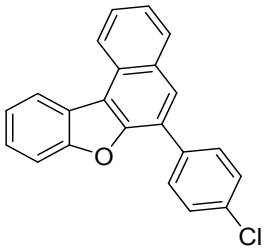	**2**{*2,7*} (89)
11	**1**{*3*}	**3**{*10*}	**4**{*3,10*} (62)	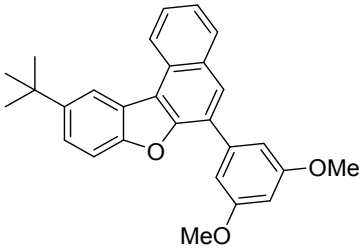	**2**{*3,10*} (95)
12	**1**{*3*}	**3**{*4*}	**4**{*3,4*} (79)	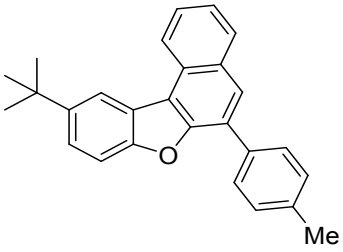	**2**{*3,4*} (88)
13	**1**{*4*}	**3**{*3*}	**4**{*4,3*} (81)	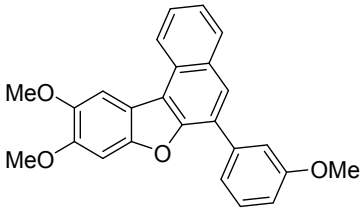	**2**{*4,3*} (92)
14	**1**{*4*}	**3**{*11*}	**4**{*4,11*} (93)	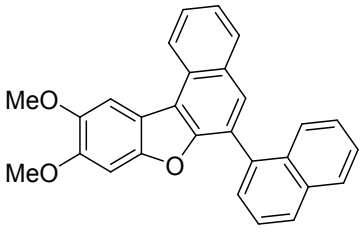	**2**{*4,11*} (78)

15	**1**{*4*}	**3**{*12*}	**4**{*4,12*} (81)	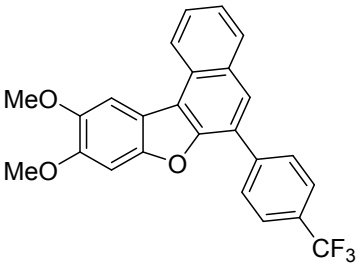	**2**{*4,12*} (86)
16	**1**{*5*}	**3**{*1*}	**4**{*5,1*} (94)	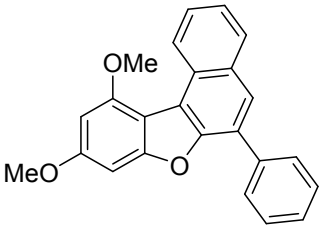	**2**{*5,1*} (84)
17	**1**{*5*}	**3**{*13*}	**4**{*5,13*}[c] (69)	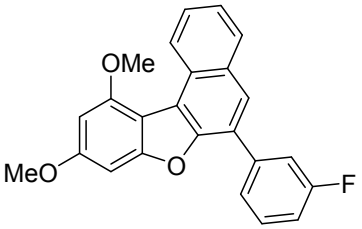	**2**{*5,13*} (65)
18	**1**{*6*}	**3**{*1*}	**4**{*6,1*}[c] (62)	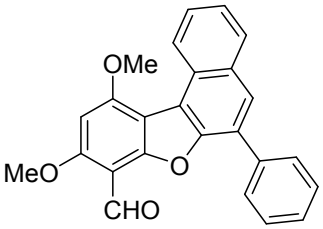	**2**{*6,1*} (77)
19	**1**{*6*}	**3**{*2*}	**4**{*6,2*}[c] (65)	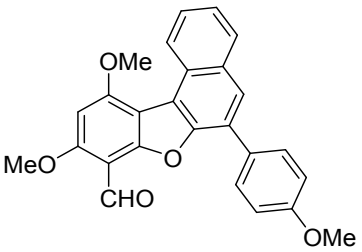	**2**{*6,2*} (76)

[a] A mixture of **1**, terminal alkyne (1.1 equiv), $(Ph_3P)_2PdCl_2$ (0.1 equiv), CuI (0.1 equiv) in Et_3N was stirred at 80 °C. A solution of **4** in TFA/DCE (1/2) was heated at 80 °C for 1 h. [b] Isolated yield (%). [c] DIPEA/DMF (1/2) was used instead of Et_3N.

With the synthesized compounds in hand, we investigated the optical properties of the naphtho[2,1-*b*]benzofurans series and summarized the absorption and emission maxima along with the quantum yields in Table 2. Figure 3 depicts the UV/Vis absorption and emission spectra of representative compounds. The absorption maxima of the compounds were observed

at approximately 300−350 nm, whereas emission maxima were observed at approximately 380−450 nm in DMSO. The observed large Stokes shift up to 100 nm that avoids reabsorption of emitted photons is a critical parameter for bioimaging applications. Structure-property relationship analysis based on the optical properties revealed that electron-donating -OCH_3 groups attached to the A ring increased the redshifts of emission spectra, whereas the electron-withdrawing groups (-Cl and -CF_3) in the E ring resulted in a redshift of emission maxima (Figure S1).

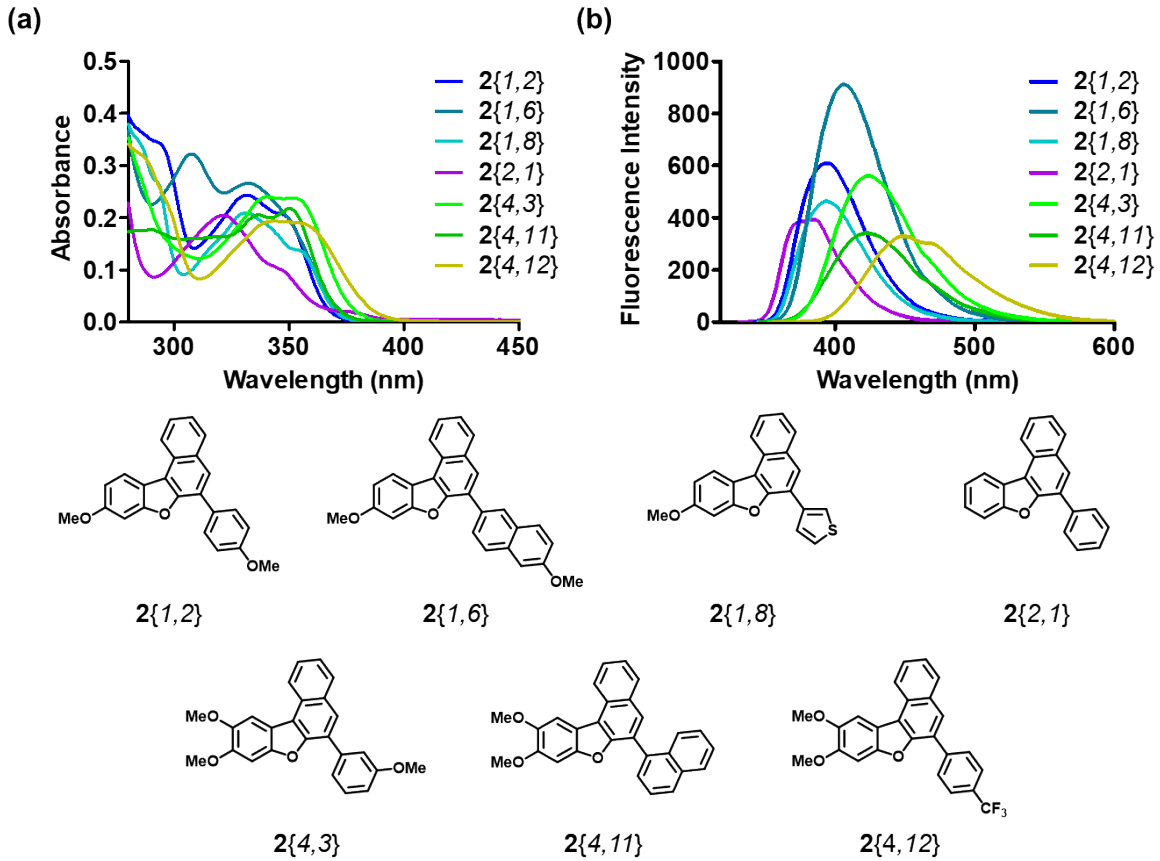

Figure 3. Absorption **(a)** and emission **(b)** spectra of **2**{*1,2*}, **2**{*1,6*}, **2**{*1,8*}, **2**{*2,1*}, **2**{*4,3*}, **2**{*4,11*}, and **2**{*4,12*} measured in DMSO.

Compound	λ_{abs} (nm)	λ_{em} (nm)			ε_{max} ($M^{-1}cm^{-1}$)	Φ_F (Solution)
		DW	EtOH	DMSO		
2{*1,1*}	329	420.5	389.5	400.5	18600	0.60
2{*1,2*}	331	412.5	384.5	393.5	23200	0.74
2{*1,3*}	328	413.5	390.5	401.5	18600	0.67
2{*1,4*}	328	431.5	388	397.5	18800	0.62
2{*1,5*}	329	411.5	389	399.5	18800	0.57
2{*1,6*}	308	425.5	393.5	406	32800	0.78
2{*1,7*}	328	430.5	393.5	408.5	17900	0.63
2{*1,8*}	332	412.5	385.5	394	20100	0.63
2{*2,1*}	321	380	379.5	384.5	19300	0.38
2{*2,7*}	322	386	383.5	388.5	21700	0.45
2{*3,10*}	325	392	382.5	387	14400	0.39
2{*3,4*}	324	406	379.5	383.5	21800	0.51
2{*4,3*}	342	435.5	404.5	425	22800	0.66
2{*4,11*}	350	426.5	402	423	20700	0.70
2{*4,12*}	355	447.5	424.5	449	18400	0.72
2{*5,1*}	322	444.5	398.5	412	15900	0.52
2{*5,13*}	322	452	405.5	423	14900	0.58
2{*6,1*}	354	-	478	-	15400	0.06
2{*6,2*}	311	473.5	487	424.5	22100	0.03

Table 2. Optical properties of 6-substituted naphtho[2,1-*b*]benzofurans.

By using a high-content imaging system, we also screened the synthesized compounds for live cell imaging in HeLa cells and the compounds **2**{*4,3*}, **2**{*4,12*}, and **2**{*5,13*} were found to be the most cell permeable, located in the cytosol of HeLa cell (Figure S2 and Figure S3). Meanwhile, **2**{*1,6*} and **2**{*1,8*} exhibited high fluorescence via aggregation induced emission properties. The phototoxicities of these compounds were found to be negligible (Figure S4). Figure 4 depicts DSE properties of **2**{*1,6*}, **2**{*1,8*}, and **2**{*4,3*}. The increase of water contents

resulted in fluorescence enhancement up to 70% of water in THF, but fluorescence decrease was observed at > 70% of water contents. These compounds possessed high QYs in ethanol solution and in solid states (Figure 5 and Table 3). DLS analysis showed that the particle sizes of **2**{*1,6*}, **2**{*1,8*}, **2**{*4,3*}, and **2**{*4,12*} are 211 nm, 208 nm, 167 nm, and 200 nm, respectively (Figure S5). In addition, they exhibited high fluorescence in most solvents, except water (Figure S6).

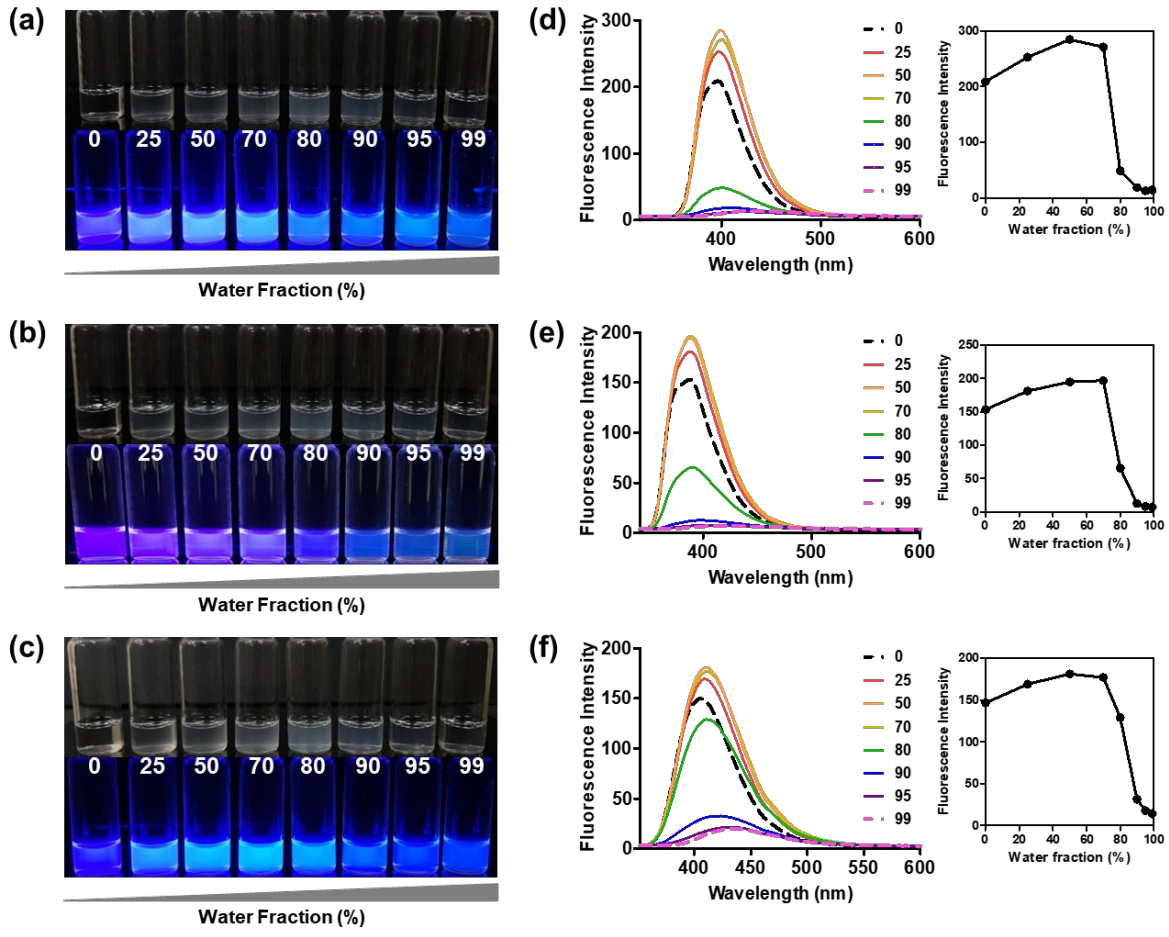

Figure 4. Photographs of 10 μM **2**{*1,6*} **(a)**, **2**{*1,8*} **(b)**, and **2**{*4,3*} **(c)** in THF/water mixture (0-99%) under natural light (up) and UV light (down, λ_{ex} = 312 nm). Fluorescence spectra of 10 μM **2**{*1,6*} **(d)**, **2**{*1,8*} **(e)**, and **2**{*4,3*} **(f)** in THF/water mixture (0-99%) with excitation at 308 nm **(d)**, at 332 nm **(e)**, and at 342 nm **(f)**; inset: plots of fluorescence intensity of **2**{*1,6*} at 396 nm **(d)**, **2**{*1,8*} at 388 nm **(e)**, and **2**{*4,3*} at 405 nm **(f)**.

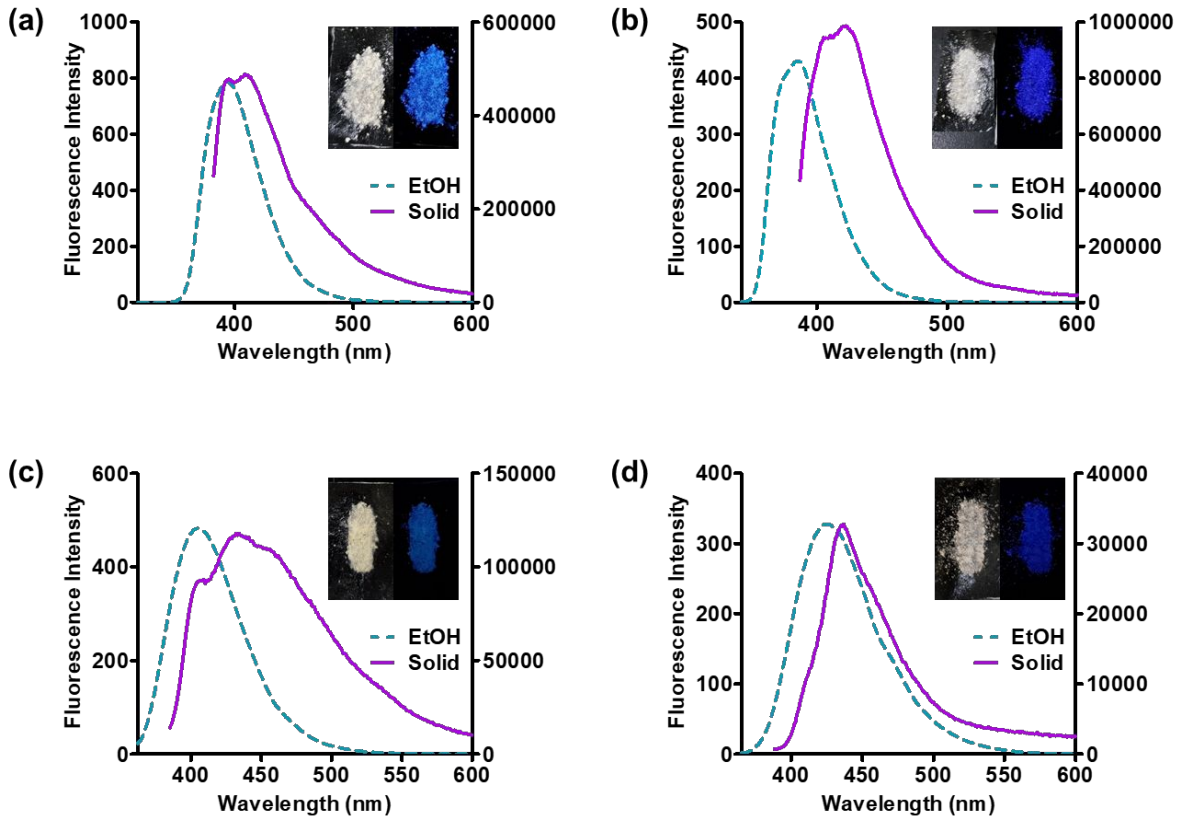

Figure 5. Fluorescence spectra of **2**{*1,6*} **(a)**, **2**{*1,8*} **(b)**, **2**{*4,3*} **(c)**, and **2**{*4,12*} **(d)** in EtOH (0.5 μM, dashed line) and solid states (solid line); inset: photographs of **2**{*1,6*} **(a)**, **2**{*1,8*} **(b)**, **2**{*4,3*} **(c)**, and **2**{*4,12*} **(d)** in the solid state under visible light (left) and UV light (right, λ_{ex} = 365 nm).

Compound	EtOH			Solid		
	λ_{abs} (nm)	λ_{em} (nm)	Φ_F (Solution)	λ_{abs} (nm)	λ_{em} (nm)	Φ_F (Solid, %)
2{*1,6*}	308	393.5	0.78	367	408	19.67
2{*1,8*}	332	385.5	0.63	372	422	22.15
2{*4,3*}	342	404.5	0.66	370	434	16.33
2{*4,12*}	355	424.5	0.72	373	437	1.54

Table 3. Optical properties of **2**{*1,6*}, **2**{*1,8*}, **2**{*4,3*}, and **2**{*4,12*} in ethanol and in the solid state.

To understand the interactions that contributed to solid state emission, we also investigated the intermolecular interactions of **2**{*1,8*} by analyzing the geometry and packing arrangements in crystal states (Figure 6). One of the featured interactions in **2**{*1,8*} packing is slip-stacks,[64] in which the intermolecular distance between 6-arylnaphtho[2,1-*b*]benzofuran rings from each centroid was 5.729 Å with a pitch angle of 54.711°, much deviated from conventional π-π stacking interactions that cause fluorescence decreases. Through the slip-stacks, each **2**{*1,8*} compound is arranged to have a short distance between S atoms of the thienyl group. The intermolecular S···S interaction (3.769 Å) along with nonclassical hydrogen bonds (CH···O bond: 2.524 Å; CH···S bond: 3.156 Å) comprise the intermolecular networks, rigidifying the molecular packing of **2**{*1,8*} as depicted in Figure 6. These intermolecular hydrogen bonds in addition to the well-aligned O and S atoms had significant influence on the molecular packing mode, resulting in high emission in solid states.[65] These nonbonding interactions are found to extend electronic communication, leading to a radiative pathway.[66]

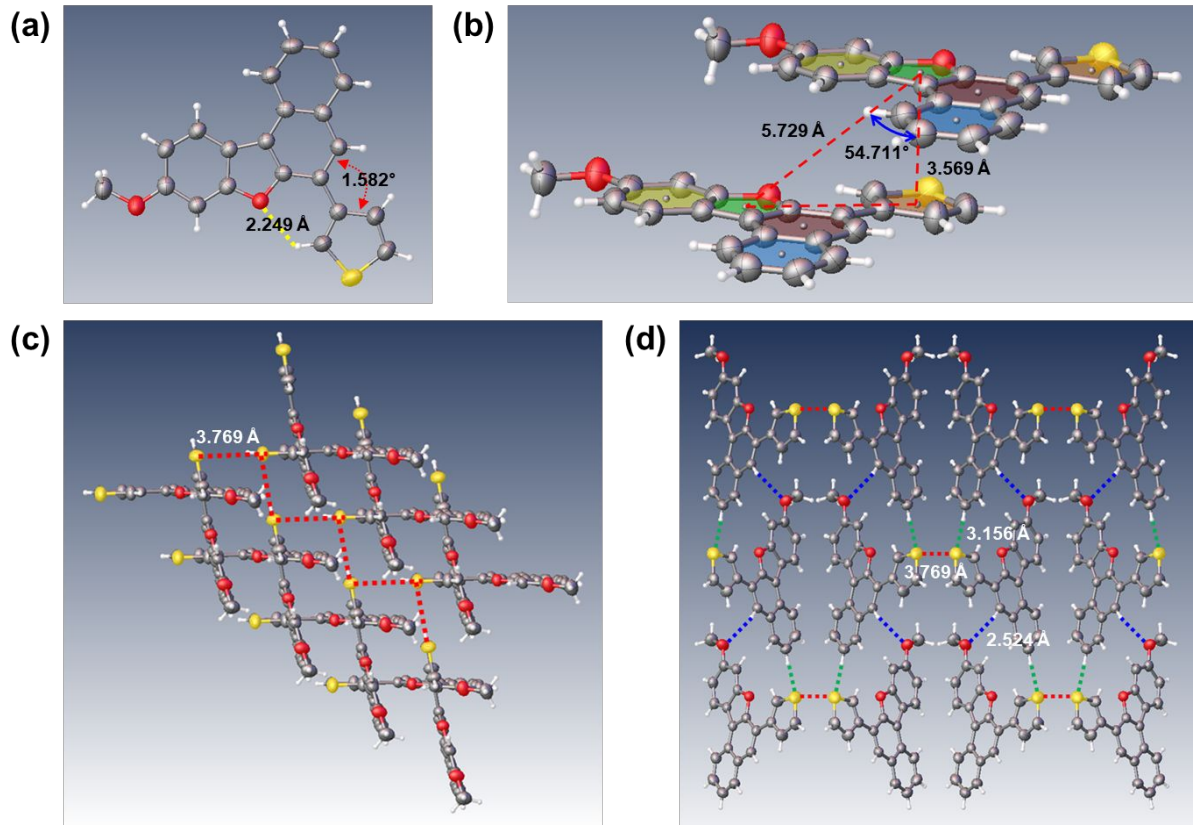

Figure 6. (a) Crystal structure of **2**{*1,8*} with the intramolecular CH···O interaction (2.249 Å) shown in yellow line. **(b)** Slip-stacked **2**{*1,8*} molecules from a side view. **(c)** Packing structure of **2**{*1,8*} via intermolecular S···S bond (3.769 Å) shown in red line. **(d)** Packing structure of **2**{*1,8*} via intermolecular interactions; red: intermolecular S···S bond (3.769 Å); green: intermolecular CH···S bond (3.156 Å); blue: intermolecular CH···O bond (2.524 Å).

In conclusion, we have developed a modular approach to a wide range of 6-substituted naphtho[2,1-*b*]benzofurans by way of sequential Sonogashira cross-coupling and 6-endo-dig electrophilic cyclization. The synthesized compounds were tested for their optical and imaging properties. By using a high-content imaging system, **2**{*4,3*}, **2**{*4,12*}, and **2**{*5,13*} were found to be the most cell permeable, whereas **2**{*1,6*} and **2**{*1,8*} exhibited high fluorescence via aggregation-induced emission properties. Interestingly, **2**{*1,6*}, **2**{*1,8*}, and **2**{*4,3*} are solid-state emissive and highly fluorescent in most solvents in solution, exhibiting dual state emission (DSE) properties that are highly valuable for broad applications including bioimaging.

The compounds we developed in this work would serve as a novel fluorescent scaffold with a variety of biomedical and optoelectronic applications.

Experimental procedures

General Methods

Unless specified, all reagents and starting materials were purchased from commercial sources and used as received without purification. "Concentrated" refers to the removal of volatile solvents via distillation using a rotary evaporator. "Dried" refers to pouring onto, or passing through, anhydrous magnesium sulfate followed by filtration. Flash chromatography was performed using silica gel (230−400 mesh) with hexanes, ethyl acetate, and dichloromethane as the eluents. All reactions were monitored by thin-layer chromatography on 0.25 mm silica plates (F-254) visualizing with UV light. Melting points were measured using a capillary melting point apparatus. ^{1}H and ^{13}C NMR spectra were recorded on 400 MHz NMR spectrometer and were described as chemical shifts, multiplicity (s, singlet; d, doublet; t, triplet; q, quartet; m, multiplet), coupling constant in hertz (Hz), and number of protons. HRMS was measured with electrospray ionization (ESI) and Q-TOF mass analyzer.

Synthesis of 6-methoxy-3-(2-(phenylethynyl)phenyl)benzofuran (**4**{*1,1*}**)**

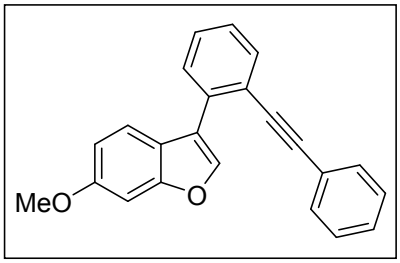

In a vial charged with 3-(2-iodophenyl)-6-methoxybenzofuran **(1**{*1*}**)** (50 mg, 0.14 mmol) in Et_3N (2 mL) were added phenylacetylene **(3**{*1*}**)**(17 µL, 0.154 mmol), $(Ph_3P)_2PdCl_2$ (9.8 mg, 0.014 mmol), and CuI (2.7 mg, 0.014 mmol). After being stirred at 80 °C for 12 h, the reaction mixture was concentrated *in vacuo* to

yield the crude product. Purification by flash chromatography on silica gel (hexanes:EtOAc, 49:1) afforded **4**{*1,1*} as a yellow gum (40.6 mg, 88%). **^{1}H NMR** (400 MHz, $CDCl_3$) δ 7.99 (s, 1H), 7.71 (d, *J* = 7.6 Hz, 1H), 7.61-7.64 (m, 2H), 7.44 (t, *J* = 7.6 Hz, 1H), 7.36 (t, *J* = 7.2 Hz, 1H), 7.29 (s, 5H), 7.11 (s, 1H), 6.94 (dd, *J* = 2.0, 8.8 Hz, 1H), 3.89 (s, 3H); **^{13}C NMR** (100 MHz, $CDCl_3$) δ 158.2, 156.3, 142.8, 134.0, 133.4, 131.5, 129.4, 128.7, 128.4, 128.4, 127.3, 123.3, 122.2, 121.3, 120.5, 120.4, 112.1, 96.2, 93.1, 89.4, 55.9; **HRMS** (ESI-QTOF) *m/z* $[M+H]^+$ calcd for $C_{23}H_{17}O_2$ 325.1223, found 325.1225.

Synthesis of 9-methoxy-6-phenylnaphtho[2,1-*b*]benzofuran (2{*1,1*})

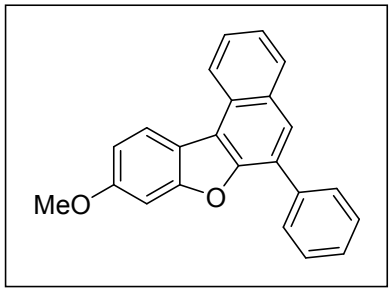

A solution of **4**{*1,1*} (25 mg, 0.08 mmol) in a mixture of DCE (2.0 mL) and TFA (1.0 mL) in a vial was stirred at 80 °C for 30 min. After being cooled down to rt, the reaction mixture was concentrated *in vacuo* to afford the crude product which was purified by flash chromatography on silica gel (hexanes:EtOAc, 49:1) to give **2**{*1,1*} as a pale yellow solid, (23.2 mg, 93%); mp: 93.7-95.2 °C; **^{1}H NMR** (400 MHz, $CDCl_3$) δ 8.58 (d, *J* = 8.4 Hz, 1H), 8.29 (d, *J* = 8.4 Hz, 1H), 8.05 (d, *J* = 8.0 Hz, 1H), 7.99 (d, *J* = 8.0 Hz, 2H), 7.95 (s, 1H), 7.69 (t, *J* = 6.8 Hz, 1H), 7.53-7.61 (m, 3H), 7.48 (t, *J* = 7.6 Hz, 1H), 7.25 (d, *J* = 2.0 Hz, 1H), 7.10 (dd, *J* = 2.0, 8.8 Hz, 1H), 3.93 (s, 3H); **^{13}C NMR** (100 MHz, $CDCl_3$) δ 159.2, 157.4, 152.1, 136.7, 131.0, 129.4, 129.2, 128.8, 128.2, 128.1, 126.9, 126.9, 126.2, 124.8, 123.4, 122.4, 118.4, 118.4, 112.0, 96.8, 55.9; **HRMS** (ESI-QTOF) *m/z* $[M+H]^+$ calcd for $C_{23}H_{17}O_2$ 325.1223, found 325.1226.

Optical characterization

The UV-Vis absorption spectra of the synthesized compounds were measured at ambient temperature using a Lambda25 UV/Vis spectrometer (PerkinElmer, Waltham, MA, USA). Fluorescence emission spectra were obtained with an FP-6500 spectrofluorometer (JASCO, Tokyo, Japan) with slit widths of 3 nm for excitation and 5 nm for emission. The solid state fluorescence emission spectra were measured at room temperature using a Fluoromax-4 spectrofluorometer (Horiba Jobin Yvon, Kyoto, Japan) with a slit width of 0.5 nm for both excitation and emission. Fluorescence quantum yields of the compounds in solution were determined using anthracene ($\Phi = 0.27$ in EtOH) as a standard and the absolute fluorescence quantum yields of solids were measured using a Horiba FluoroMax-4 spectrofluorometer with an integrating sphere assembly. Dynamic light scattering was employed to analyze the particle size distribution using ELSZ-2000 (Otsuka, Chiyoda, Japan).

Image-based cell screening

HeLa (human cervical cancer cell line) cells were seeded at 20,000 cells per well in a Cellcarrier-96 black plate (PerkinElmer, Waltham, MA, USA) and incubated for 24 h at 37 °C in 5% CO_2. For live cell imaging, the cells were treated with the compounds for 1 h and cell screening images were acquired via the Operetta High-Content imaging system (PerkinElmer, Waltham, MA, USA) at 410-480 nm with blue fluorescence upon excitation at 360-400 nm with a 20x objective lens. Image analysis was performed using Harmony software (PerkinElmer, Waltham, MA, USA).

Confocal microscopy

For live cell imaging, HeLa cells were seeded on a confocal dish for 24 h under 37 °C in 5% CO_2. After incubation, the same samples were incubated with 10 μM NP compounds for 1 h at 37 °C under 5% CO_2, followed by staining with 150 nM MitoTracker Red (Molecular probes, Eugene, OR, USA) for 20 min or with 75 nM LysoTracker Red (Molecular probes, Eugene, OR, USA) for 30 min. After staining, the samples were washed twice with Dulbecco's phosphate-buffered saline (DPBS) and live cell imaging was carried out using a TCS-SP8 confocal laser scanning microscope (Leica, Wetzlar, Germany). Cell images of NP-treated cells were acquired at 410-560 nm with blue fluorescence upon excitation at 405 nm, whereas LysoTracker Red and MitoTracker Red were excited at 561 nm and detected at >566 nm with red fluorescence.

Cytotoxicity test

The phototoxicity of the compounds was evaluated using the MTT assay. MCF7 (human breast cancer cell line) cells were seeded in 96-well cell culture plates (SPL Life Science Co., Gyeonggi-do, Republic of Korea) at a density of 10,000 cells per well. After incubation for 24 h, the cells were treated with different concentrations (0.5, 1, 2, 5, and 10 μM) of compounds in cell culture media for 1 h at 37 °C in the dark. The cell medium was replaced with fresh medium and cells were then irradiated by a blue LED light (800 lm/m^2) for 0, 5, and 10 min. After illumination, the cells were incubated at 37 °C under 5% CO_2 in the dark for 24 h. After medium replacement, 20 μM 3-(4,5-dimethylthiazol-2-yl)-2,5-diphenyltetrazolium bromide (MTT) (5 mg/mL) was added to each well and incubated for another 3 h. At the end, the

medium was removed and the formazan product was dissolved in DMSO (100 μL per well). Cell viability was evaluated by measuring the absorbance at 570 nm using a Mithras^2 plate reader (Berthold Technologies, Bad Wildbad, Germany).

Single Crystal X-ray Diffraction Studies

Single crystals of **2**{*1,8*} with a dimension of 0.427 × 0.22 × 0.104 mm^3 were grown by the vapor diffusion method using CH_2Cl_2 and cyclopentane. The suitable crystal was mounted on SuperNova, Dual, Cu at home/near, and a AtlasS2 diffractometer (Agilent, Santa Clara, CA, USA). The data collection of **2**{*1,8*} was performed using a SuperNova dual source diffractometer operating with Cu-K_α radiation (λ = 1.542 mm^{-1}) at 294.4 K. Using Olex2,[67] the structure was solved by direct methods with ShelXT software[68] and refined by the least squares minimization method using ShelXL software.[69] Supplementary crystallographic data of **2**{*1,8*} in this paper can be obtained from the Cambridge Crystallographic Data Centre via www.ccdc.cam.ac.uk/data_request/cif. The deposition number of **2**{*1,8*} is CCDC 1884862. All copies of the data can be downloaded upon request to CCDC, 12 Union Road, Cambridge CB2 1EZ, UK.

Author information

Corresponding authors

* I. Kim: e-mail: ikyonkim@yonsei.ac.kr; fax: +82 32 749 4105

* J. Lee: e-mail: jyleeut@snu.ac.kr; fax: +82 2 884 8334

The authors declare no competing financial interest.

Acknowledgements

This work was supported by the National Research Foundation of Korea (NRF) grant funded by the Korea government (MSIP) (NRF-2017R1A2A2A05069364 and NRF-2018R1A6A1A03023718) to I. K.; the National Research Foundation of Korea (NRF) grants funded by the Korean government (MSIP) (NRF-2018R1A2B2005535 and 2018R1A4A1021703) to J. L.

Abbreviations

ACQ: aggregation-caused quenching

AIE: aggregation-induced emission

AIEE: aggregation-induced emission enhancement

DSE: dual state emission

DPBS: Dulbecco's phosphate-buffered saline

MTT: 3-(4,5-dimethylthiazol-2-yl)-2,5-diphenyltetrazolium bromide

NP: naphtho[2,1-*b*]benzofuran

QY: quantum yields

RIR: restricted intramolecular rotation

Supporting Information

^{1}H and ^{13}C NMR spectra of synthesized compounds, compound synthesis and characterization data, supporting figures, and crystal structure determination of **2**{*1,8*}.

References

1. For a recent review, see: Stepien, M.; Gonka, E.; Zyla, M.; Sprutta, N., Heterocyclic Nanographenes and Other Polycyclic Heteroaromatic Compounds: Synthetic Routes, Properties, and Applications. *Chem Rev* **2017,** *117* (4), 3479-3716.

2. Hamasaki, A.; Zimpleman, J. M.; Hwang, I.; Boger, D. L., Total synthesis of ningalin D. *J Am Chem Soc* **2005,** *127* (30), 10767-10770.

3. Rao, H. S. P.; Vijjapu, S., Synthesis and photochromic properties of benzofuran-phenanthrene and benzofuran-pyrene hybrids. *Rsc Adv* **2014,** *4* (49), 25747-25758.

4. Park, S.; Kwon, D. I.; Lee, J.; Kim, I., When Indolizine Meets Quinoline: Diversity-Oriented Synthesis of New Polyheterocycles and Their Optical Properties. *ACS Comb Sci* **2015,** *17* (8), 459-469.

5. Suh, S. E.; Barros, S. A.; Chenoweth, D. M., Triple Aryne-Tetrazine Reaction Enabling Rapid Access to a New Class of Polyaromatic Heterocycles. *Chem Sci* **2015,** *6*, 5128-5132.

6. Wang, S.; Lv, B.; Cui, Q.; Ma, X.; Ba, X.; Xiao, J., Synthesis, Photophysics, and Self-Assembly of Furan-Embedded Heteroarenes. *Chemistry* **2015,** *21* (42), 14791-14796.

7. Kaida, H.; Goya, T.; Nishii, Y.; Hirano, K.; Satoh, T.; Miura, M., Construction of Bisbenzofuro[2,3-b:3',2'-e]pyridines by Palladium-Catalyzed Double Intramolecular Oxidative C-H/C-H Coupling. *Org Lett* **2017,** *19* (5), 1236-1239.

8. Beija, M.; Afonso, C. A.; Martinho, J. M., Synthesis and applications of Rhodamine derivatives as fluorescent probes. *Chem Soc Rev* **2009,** *38* (8), 2410-2433.

9. Guo, Z.; Park, S.; Yoon, J.; Shin, I., Recent progress in the development of near-infrared fluorescent probes for bioimaging applications. *Chem Soc Rev* **2014,** *43* (1), 16-29.

10. Kowada, T.; Maeda, H.; Kikuchi, K., BODIPY-based probes for the fluorescence imaging of biomolecules in living cells. *Chem Soc Rev* **2015,** *44* (14), 4953-4972.

11. Zong, L. Y.; Xie, Y. J.; Wang, C.; Li, J. R.; Li, Q. Q.; Li, Z., From ACQ to AIE: the suppression of the strong pi-pi interaction of naphthalene diimide derivatives through the adjustment of their flexible chains. *Chem Commun* **2016,** *52* (77), 11496-11499.

12. Sasaki, S.; Suzuki, S.; Sameera, W. M. C.; Igawa, K.; Morokuma, K.; Konishi, G., Highly Twisted N,N-Dialkylamines as a Design Strategy to Tune Simple Aromatic Hydrocarbons as Steric Environment-Sensitive Fluorophores. *J Am Chem Soc* **2016,** *138* (26), 8194-8206.

13. Huang, M.; Yu, R.; Xu, K.; Ye, S.; Kuang, S.; Zhu, X.; Wan, Y., An arch-bridge-type fluorophore for bridging the gap between aggregation-caused quenching (ACQ) and aggregation-induced emission (AIE). *Chem Sci* **2016,** *7* (7), 4485-4491.

14. Hong, Y. N.; Lam, J. W. Y.; Tang, B. Z., Aggregation-induced emission. *Chem Soc Rev* **2011,** *40* (11), 5361-5388.

15. Mei, J.; Leung, N. L. C.; Kwok, R. T. K.; Lam, J. W. Y.; Tang, B. Z., Aggregation-Induced Emission: Together We Shine, United We Soar! *Chem Rev* **2015,** *115* (21), 11718-11940.

16. Li, Q. Q.; Li, Z., The Strong Light-Emission Materials in the Aggregated State: What Happens from a Single Molecule to the Collective Group. *Adv Sci* **2017,** *4* (7), 1600484, 1-15.

17. Shi, J. Q.; Suarez, L. E. A.; Yoon, S. J.; Varghese, S.; Serpa, C.; Park, S. Y.; Luer, L.; Roca-Sanjuan, D.; Milian-Medina, B.; Gierschner, J., Solid State Luminescence Enhancement in a pi-Conjugated Materials: Unraveling the Mechanism beyond the Framework of AIE/AIEE. *J Phys Chem C* **2017,** *121* (41), 23166-23183.

18. An, B. K.; Kwon, S. K.; Jung, S. D.; Park, S. Y., Enhanced emission and its switching in fluorescent organic nanoparticles. *J Am Chem Soc* **2002,** *124* (48), 14410-14415.

19. Qin, W.; Ding, D.; Liu, J. Z.; Yuan, W. Z.; Hu, Y.; Liu, B.; Tang, B. Z., Biocompatible Nanoparticles with Aggregation-Induced Emission Characteristics as Far-Red/Near-Infrared Fluorescent Bioprobes for In Vitro and In Vivo Imaging Applications. *Adv Funct Mater* **2012,** *22* (4), 771-779.

20. Beppu, T.; Tomiguchi, K.; Masuhara, A.; Pu, Y. J.; Katagiri, H., Single Benzene Green Fluorophore: Solid-State Emissive, Water-Soluble, and Solvent- and pH-Independent Fluorescence with Large Stokes Shifts. *Angew Chem Int Ed Engl* **2015,** *54* (25), 7332-7335.

21. Li, M.; Niu, Y.; Zhu, X.; Peng, Q.; Lu, H. Y.; Xia, A.; Chen, C. F., Tetrahydro[5]helicene-based imide dyes with intense fluorescence in both solution and solid state. *Chem Commun (Camb)* **2014,** *50* (23), 2993-2995.

22. Gopikrishna, P.; Iyer, P. K., Monosubstituted Dibenzofulvene-Based Luminogens: Aggregation Induced Emission Enhancement and Dual-State Emission. *J Phys Chem C* **2016,** *120* (46), 26556-26568.

23. Raghuvanshi, A.; Jha, A. K.; Sharma, A.; Umar, S.; Mishra, S.; Kant, R.; Goel, A., A Nonarchetypal 5,6-Dihydro-2H-pyrano[3,2-g]indolizine-Based Solution-Solid Dual Emissive

AIEgen with Multicolor Tunability. *Chemistry* **2017,** *23* (19), 4527-4531.

24. Mei, X.; Wang, J.; Zhou, Z.; Wu, S.; Huang, L.; Lin, Z.; Ling, Q., Diarylmaleic anhydrides: unusual organic luminescence, multi-stimuli response and photochromism. *J Mater Chem C* **2017,** *5* (8), 2135-2141.

25. Wang, J.; Liu, Z.; Yang, S.; Lin, Y.; Lin, Z.; Ling, Q., Large Changes in Fluorescent Color and Intensity of Symmetrically Substituted Arylmaleimides Caused by Subtle Structure Modifications. *Chemistry* **2018,** *24* (2), 322-326.

26. Liu, Y. W.; Zhang, Y.; Wu, X. H.; Lan, Q.; Chen, C. S.; Liu, S. W.; Chi, Z. G.; Jiang, L.; Chen, X. D.; Xu, J. R., Deep-blue luminescent compound that emits efficiently both in solution and solid state with considerable blue-shift upon aggregation. *J Mater Chem C* **2014,** *2* (6), 1068-1075.

27. Li, W. J.; Liu, D. D.; Shen, F. Z.; Ma, D. G.; Wang, Z. M.; Feng, T.; Xu, Y. X.; Yang, B.; Ma, Y. G., A Twisting Donor-Acceptor Molecule with an Intercrossed Excited State for Highly Efficient, Deep-Blue Electroluminescence. *Adv Funct Mater* **2012,** *22* (13), 2797-2803.

28. Liu, B.; Yuan, Y.; He, D.; Huang, D. Y.; Luo, C. Y.; Zhu, Z. L.; Lu, F.; Tong, Q. X.; Lee, C. S., High-Performance Blue OLEDs Based on Phenanthroimidazole Emitters via Substitutions at the C6-and C9-Positions for Improving Exciton Utilization. *Chem-Eur J* **2016,** *22* (34), 12130-12137.

29. Kumar, S.; Singh, P.; Kumar, P.; Srivastava, R.; Pal, S. K.; Ghosh, S., Exploring an Emissive Charge Transfer Process in Zero-Twist Donor-Acceptor Molecular Design as a Dual-State Emitter. *J Phys Chem C* **2016,** *120* (23), 12723-12733.

30. Beppu, T.; Tomiguchi, K.; Masuhara, A.; Pu, Y. J.; Katagiri, H., Single Benzene Green Fluorophore: Solid-State Emissive, Water-Soluble, and Solvent-and pH-Independent Fluorescence with Large Stokes Shifts. *Angew Chem Int Edit* **2015,** *54* (25), 7332-7335.

31. Huang, M.; Zhou, J.; Xu, K.; Zhu, X.; Wan, Y., Enhancement of the excited-state intramolecular proton transfer process to produce all-powerful DSE molecules for bridging the gap between ACQ and AIE. *Dyes and Pigments* **2019,** *160*, 839-847.

32. Kwon, S.; Kwon, D. I.; Jung, Y.; Kim, J. H.; Lee, Y.; Lim, B.; Kim, I.; Lee, J., Indolizino[3,2-c]quinolines as environment-sensitive fluorescent light-up probes for targeted live cell imaging. *Sensor Actuat B-Chem* **2017,** *252*, 340-352.

33. Kim, I.; Choi, J., A versatile approach to oligostilbenoid natural products--synthesis

of permethylated analogues of viniferifuran, malibatol A, and shoreaphenol. *Org Biomol Chem* **2009,** *7* (13), 2788-2795.

34. Kim, I.; Kim, K.; Choi, J., A direct approach to 5-hydroxybenzofurans via a platinum-catalyzed domino rearrangement/5-endo-dig cyclization reaction of quinols. *J Org Chem* **2009,** *74* (21), 8492-8495.

35. Kim, K.; Kim, I., Total synthesis of diptoindonesin G via a highly efficient domino cyclodehydration/intramolecular Friedel-Crafts acylation/regioselective demethylation sequence. *Org Lett* **2010,** *12* (22), 5314-5317.

36. Lee, S. H.; Kim, I.; Kim, S. H., Anti-resorptive and Anabolic Activity of 3-(3,5-Dimethoxyphenyl)-6-methoxybenzofuran-4-carboxylate. *B Korean Chem Soc* **2011,** *32* (11), 4137-4140.

37. Lee, J. H.; Kim, M.; Kim, I., Palladium-catalyzed alpha-arylation of aryloxyketones for the synthesis of 2,3-disubstituted benzofurans. *J Org Chem* **2014,** *79* (13), 6153-6163.

38. Nayak, M.; Jung, Y.; Kim, I., Syntheses of pterocarpenes and coumestans via regioselective cyclodehydration. *Org Biomol Chem* **2016,** *14* (34), 8074-8087.

39. Jung, Y.; Kim, I., Chemoselective reduction of quinols as an alternative to Sonogashira coupling: synthesis of polysubstituted benzofurans. *Org Biomol Chem* **2016,** *14* (44), 10454-10472.

40. Nayak, M.; Singh, D. K.; Kim, I., Polyaromatic heterocycles through intramolecular alkyne carbonyl metathesis: 5-Acylnaphtho[2,1-b]benzofurans. *Tetrahedron* **2017,** *73* (14), 1831-1840.

41. Nayak, M.; Singh, D. K.; Kim, I., Regiospecific Synthesis of 5-and 6-Acylated Naphtho[1,2-b]benzofurans via Intramolecular Alkyne Carbonyl Metathesis. *Synthesis-Stuttgart* **2017,** *49* (9), 2063-2073.

42. Sonogashira, K.; Tohda, Y.; Hagihara, N., Convenient Synthesis of Acetylenes - Catalytic Substitutions of Acetylenic Hydrogen with Bromoalkenes, Iodoarenes, and Bromopyridines. *Tetrahedron Lett* **1975,** (50), 4467-4470.

43. Sonogashira, K., Development of Pd-Cu catalyzed cross-coupling of terminal acetylenes with sp(2)-carbon halides. *J Organomet Chem* **2002,** *653* (1-2), 46-49.

44. Negishi, E.; Anastasia, L., Palladium-catalyzed alkynylation. *Chem Rev* **2003,** *103* (5), 1979-2017.

45. Chinchilla, R.; Najera, C., Recent advances in Sonogashira reactions. *Chem Soc Rev* **2011,** *40* (10), 5084-5121.

46. Larock, R. C., *Synthesis of Heterocycles and Carbocycles by Electrophilic Cyclization of Alkynes. In Acetylene Chemistry*. Diederich, F., Stang, P. J., Tykwinski, R. R. eds.; Wiley-VCH: Weinheim, Germany, 2005; p 5-99.

47. Furstner, A.; Davies, P. W., Catalytic carbophilic activation: catalysis by platinum and gold pi acids. *Angew Chem Int Ed Engl* **2007,** *46* (19), 3410-3449.

48. Yamamoto, Y.; Gridnev, I. D.; Patil, N. T.; Jin, T., Alkyne activation with Bronsted acids, iodine, or gold complexes, and its fate leading to synthetic application. *Chem Commun (Camb)* **2009,** (34), 5075-5087.

49. Godoi, B.; Schumacher, R. F.; Zeni, G., Synthesis of heterocycles via electrophilic cyclization of alkynes containing heteroatom. *Chem Rev* **2011,** *111* (4), 2937-2980.

50. Although Larock reported the synthesis of 5-iodo-6-arylnaphtho[2,1-b]benzofuran via ICl-mediated cyclization, only one example was demonstrated. See ref 55.

51. Bae, J.-S. K., J.-E.; Kim, J.-G.; Jang, J.-G. Preparation of Arenothiophenes and Related Compounds for Organic Electronic Device. WO 2010036027 A2 20100401.

52. Nakanishi, K.; Fukatsu, D.; Takaishi, K.; Tsuji, T.; Uenaka, K.; Kuramochi, K.; Kawabata, T.; Tsubaki, K., Oligonaphthofurans: fan-shaped and three-dimensional pi-compounds. *J Am Chem Soc* **2014,** *136* (19), 7101-7109.

53. Seo, S. I., T.; Ohsawa, N.; Nonaka, Y.; Sasaki, T. Light-Emitting Elements with Fluorescent and Yellow Phosphorescent Emitting Layers, and Light-Emitting Devices, Electronic Devices, and Lighting Devices Using Them. . WO 2015181667 A1 20151203.

54. Lee, B. S. C., Y. H.; Park, J. C.; Park, Y. W.; Ji, H. S.; Kang, M. S.; Yeo, S. Aromatic Heterocyclic Compounds for Organic Electronic Element and Electronic Device. . WO 2015194791 A2 20151223.

55. Yao, T.; Campo, M. A.; Larock, R. C., Synthesis of polycyclic aromatic iodides via ICl-induced intramolecular cyclization. *Org Lett* **2004,** *6* (16), 2677-2680.

56. Shi, Z.; Ding, S.; Cui, Y.; Jiao, N., A palladium-catalyzed oxidative cycloaromatization of biaryls with alkynes using molecular oxygen as the oxidant. *Angew Chem Int Ed Engl* **2009,** *48* (42), 7895-7898.

57. Baralle, A.; Yorimitsu, H.; Osuka, A., Pd-NHC-Catalyzed Alkynylation of General

Aryl Sulfides with Alkynyl Grignard Reagents. *Chemistry* **2016,** *22* (31), 10768-10772.

58. Yanagi, T.; Otsuka, S.; Kasuga, Y.; Fujimoto, K.; Murakami, K.; Nogi, K.; Yorimitsu, H.; Osuka, A., Metal-Free Approach to Biaryls from Phenols and Aryl Sulfoxides by Temporarily Sulfur-Tethered Regioselective C-H/C-H Coupling. *J Am Chem Soc* **2016,** *138* (44), 14582-14585.

59. Jacob, A.; Roy, T.; Kaicharla, T.; Biju, A. T., Metal-Free, Bronsted Acid-Catalyzed Formal [3+2] Annulation of Quinone Monoacetals with 2-Naphthols. *J Org Chem* **2017,** *82* (20), 11269-11274.

60. For synthesis of 6-aroylnaphtho[2,1-b]benzofurans, see: Paria, S.; Reiser, O., Visible Light Photoredox Catalyzed Cascade Cyclizations of alpha-Bromochalcones or alpha-Bromocinnamates with Heteroarenes. *Adv Synth Catal* **2014,** *356* (2-3), 557-562.

61. Tsuji, H.; Nakamura, E., Design and Functions of Semiconducting Fused Polycyclic Furans for Optoelectronic Applications. *Acc Chem Res* **2017,** *50* (2), 396-406.

62. Kim, I.; Lee, S. H.; Lee, S., BCl3-promoted synthesis of benzofurans. *Tetrahedron Lett* **2008,** *49* (46), 6579-6584.

63. For the synthesis of 1, see the Supporting Information.

64. Yoon, S. J.; Chung, J. W.; Gierschner, J.; Kim, K. S.; Choi, M. G.; Kim, D.; Park, S. Y., Multistimuli Two-Color Luminescence Switching via Different Slip-Stacking of Highly Fluorescent Molecular Sheets. *J Am Chem Soc* **2010,** *132* (39), 13675-13683.

65. Viglianti, L.; Leung, N. L. C.; Xie, N.; Gu, X. G.; Sung, H. H. Y.; Miao, Q.; Williams, I. D.; Licandro, E.; Tang, B. Z., Aggregation-induced emission: mechanistic study of the clusteroluminescence of tetrathienylethene. *Chem Sci* **2017,** *8* (4), 2629-2639.

66. Zhao, E.; Lam, J. W. Y.; Meng, L. M.; Hong, Y.; Deng, H. Q.; Bai, G. X.; Huang, X. H.; Hao, J. H.; Tang, B. Z., Poly[(maleic anhydride)-alt-(vinyl acetate)]: A Pure Oxygenic Nonconjugated Macromolecule with Strong Light Emission and Solvatochromic Effect. *Macromolecules* **2015,** *48* (1), 64-71.

67. Dolomanov, O. V.; Bourhis, L. J.; Gildea, R. J.; Howard, J. A. K.; Puschmann, H., OLEX2: a complete structure solution, refinement and analysis program. *J Appl Crystallogr* **2009,** *42*, 339-341.

68. Sheldrick, G. M., SHELXT - Integrated space-group and crystal-structure determination. *Acta Crystallogr A* **2015,** *71*, 3-8.

69. Sheldrick, G. M., Crystal structure refinement with SHELXL. *Acta Crystallogr C* **2015,** *71*, 3-8.